Solar Energy 194 (2019) 431–435

Contents lists available at ScienceDirect

Solar Energy

journal homepage: www.elsevier.com/locate/solener

Synthesis of new simple hole-transport materials bearing benzodithiazole based core for perovskite solar cells

T. Swetha[a,*], Mohammad Rezaul Karim[b], Hamad F. Alharbi[c], Nabeel H. Alharthi[c], B. Bais[d], Nowshad Amin[e,f], Md. Akhtaruzzaman[f,g,*]

[a] Indian Institute of Technology, Kanpur, India
[b] Center of Excellence for Research in Engineering Materials, Deanship of Scientific Research, King Saud University, Riyadh 11421, Saudi Arabia
[c] Department of Mechanical Engineering, College of Engineering, King Saud University, Riyadh 11421, Saudi Arabia
[d] Centre of Advanced Electronic and Communication Engineering (PAKET), Faculty of Engineering & Built Environment, Universiti Kebangsaan Malaysia (UKM), 43600 Bangi, Selangor, Malaysia
[e] Centre for Integrated Systems Engineering and Advanced Technologies (Integra), Faculty of Engineering and Built Environment, Universiti Kebangsaan Malaysia (UKM), 43600 Bangi, Selangor, Malaysia
[f] Institute of Sustainable Energy, Universiti Tenaga Nasional (@The National Energy University), Jalan IKRAM-UNITEN, 43000 Kajang, Selangor, Malaysia
[g] Solar Energy Research Institute, Universiti Kebangsaan Malaysia (@ The National University of Malaysia), 43600 Bangi, Selangor, Malaysia

ARTICLE INFO

Keywords:
Perovskite solar cells
Hole-transport materials (HTMs)
Photophysical properties
Benzo[c][1,2,5]thiadiazole

ABSTRACT

Benzo[c][1,2,5]thiadiazole(BT) core-based novel organic hole-transport materials (HTMs) **BTT-PMe** and **BTT-2F** are successfully synthesized for perovskite solar cells. The new HTMs are prepared by the simpler synthetic route with cost-effective purification steps. These HTMs are structurally confirmed by NMR, FT-IR and mass spectroscopy. The optical parameters are analysed using the UV–Vis spectrophotometer and cyclic voltammetry. To further confirmation of these properties we conducted the theoretical studies, which are fully matched with the experimental data. We have studied the effect of fluorine atom for its photo physical properties.

1. Introduction

Organic and inorganic perovskite solar cells (PSCs) have rapidly emerged as hottest area in the field of photovoltaic technologies, the breakthrough was done by Miyasaka et al., in 2009 (Kojima et al., 2009; Correa-Baena et al., 2017; Leijtens et al., 2017). These PSCs have reached power conversion efficiency (PCE) up to 24.2%. The PCE of PSCs is due to the proper aligned direct band gaps; broad and intensive light absorption with the high molar extinction coefficients; low exciton binding energy, long charge diffusion lengths (Ahmed et al., 2018; Chen et al., 2016) and superior charge carrier mobility of perovskites. Various PSCs have also been reported like super alkali perovskites and others to improve the photovoltaic properties (Xiaofeng et al., 2017; Tingwei et al., 2019; Tingwei et al., 2019; Tingwei et al., 2019).

The n-i-p PSCs constitutes of a conductive substrate, n-type semiconductor metal oxide, perovskite aslight-harvesting material, HTM and a metal electrode (Gao et al., 2014; Bi et al., 2016). The generated excitons in perovskite material after the incident of sunlight in PSCs diffuse to perovskite/HTM or electron transport material (ETM) interfaces and separated into holes and electrons. These separated holes and electrons move through HTM and ETM, collected by the respective electrodes. To prevent the charge recombination HTM and ETM plays a vital role. A good HTM should possess some desirable properties; high hole mobility, suitable energy levels, superior stability, good solubility, better solid-state morphology and favourable glass transition temperature (T_g). Till date 2,2′,7,7′-tetrakis(*N*,*N*-di-p-methoxyphenyl amine)-9,9′-spirobifluorene (*spiro*-OMeTAD) and PTAA (polytriarylamine) are the commercially available HTMs and showing over 22% PCE. However, the synthesis of *spiro*-OMeTAD involves multi-step, tedious synthetic routes, high cost and relatively low hole mobility in pristine form result in inferior PCE (Leijtens et al., 2012; Xu et al., 2017). Hence, the development of a new HTMs with simple synthetic protocol and less expensive is of high demand for efficient and low-cost production of PSCs. In this regard, several research groups are involved in developing cost-effective HTMs.

Till now a variety of HTMs are reported including p-type inorganic materials, such as CuSCN (Qin et al., 2014; Ye et al., 2015) or CuI (Sepalage et al., 2015) and small organic molecule HTMs (carbazole, triphenylamine, BT, fluorine, phenothiazine, S, N-heteropentacene, phenoxazine and

* Corresponding authors at: Indian Institute of Technology, Kanpur (IITK), India (T. Swetha). Solar Energy Research Institute, Universiti Kebangsaan Malaysia (UKM), Malaysia (M. Akhtaruzzaman).
E-mail addresses: swethat007@gmail.com, swetha@iitk.ac.in (T. Swetha), akhtar@ukm.edu.my (Md. Akhtaruzzaman).

https://doi.org/10.1016/j.solener.2019.10.046
Received 23 August 2019; Received in revised form 15 October 2019; Accepted 20 October 2019
Available online 07 November 2019
0038-092X/

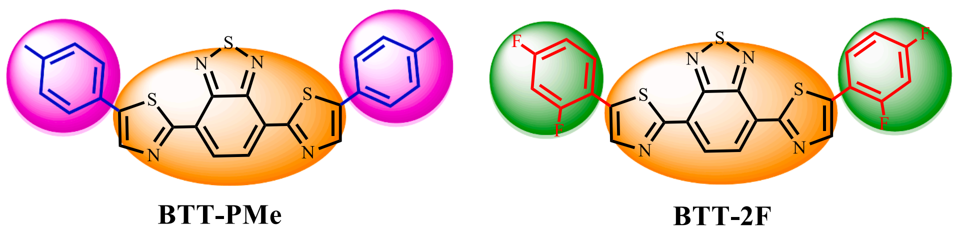

Fig. 1. Chemical structure of the synthesized novel HTMs.

pyrene core etc.,) (Cheng et al., 2016, 2017, 2018; Grisorio et al., 2017; Molina-Ontoria et al., 2016; Petrus et al., 2015; Rakstys et al., 2016). The Benzo[c] (Kojima et al., 2009; Correa-Baena et al., 2017; Chen et al., 2016) thiadiazole unit is well studied in bulk hetero-junction organic solar cells (BHJ) to improve the PCE. The central fluorinated benzene moiety HTM (DFTAB) was studied by Chen and co-workers in 2016. Linna Zhu et al. reported the BT and fluorinated BT core-based HTMs with a PCE of ~17.5 (Chen et al., 2016). Our research group is also involved in developing organic HTMs. One-step facile synthesis of a simple HTM for efficient PSCs has been reported to improve the PCE and low-cost PSCs. Recently, we have developed a very simple BT based HTMs, which have shown reasonable efficiency with suitable HOMO energy level (Swetha et al., 2018). In continuation of our work and to improve the photophysical properties, PCE and to know the effect of the fluorine atoms, we have developed two new HTMs. In this work, we have prepared **BTT-PMe** and **BTT-2F** HTMs, (Fig. 1) having 4,7-di(thiophen-2-yl)benzo[c] (Kojima et al., 2009; Correa-Baena et al., 2017; Chen et al., 2016)thiadiazole as core moiety with numerous aromatic entities. We have studied optical and electrochemical studies to know the nature of the fluorine atom.

2. Experimental section

2.1. Materials and instrumentation

The starting P-tolyl boronic acid, 2,4-difluoro phenyl boronic acid pinacol ester was obtained from Sigma-Aldrich. The solvents are purified by standard procedures and purged with nitrogen before use. Analytical grade chemicals and solvents are used in this work without further purification. UV–Visible spectra were acquired using a Shimadzu UV-1600 spectrometer in a 1 cm path length quartz cell and fluorescence spectra were recorded by using J.Y. Horiba fluorescence spectrometer. Electrochemical data were obtained by cyclic voltammetry using standard 3 eletrode system; Pt as referece and auxillary electrode, Ag/AgCl as reference electrode ona BAS100 electrochemical analyzer using 0.1 M tetrabutylammonium perchlorate as supporting electrolyte. NMR analysis were recorded in $CDCl_3$ on a Bruker 400-MHz or 500-MHz using TMS as an internal standard.

3. Theoritical calculations

Density functional theory (DFT) and time-dependent DFT calculations of these **BTT-PMe** and **BTT-2F** were performed using cam-B3LYP/6-311G* level in chloroform solution via Gaussian 09 program package (Frisch et al., 2003; Miertuš et al., 1981). To simulate the optical spectra, the lowest spin-allowed singlet-singlet transitions were computed on the ground state geometry. Transition energies, oscillator strengths and percentage contributions of the molecular orbital were interpolated by a *Gauss Sum 2.2.5.*

4. Results and discussion

4.1. Synthesis and characterization of the novel HTMs

The synthetic details are shown in the synthetic scheme. The final HTMs **BTT-Me** and **BTT-2F** were synthesized by the Suzuki-cross coupling reaction of 3 with corresponding boronic acids. These are having very high solubility in chloroform, dichloromethane and chlorobenzene solvents.

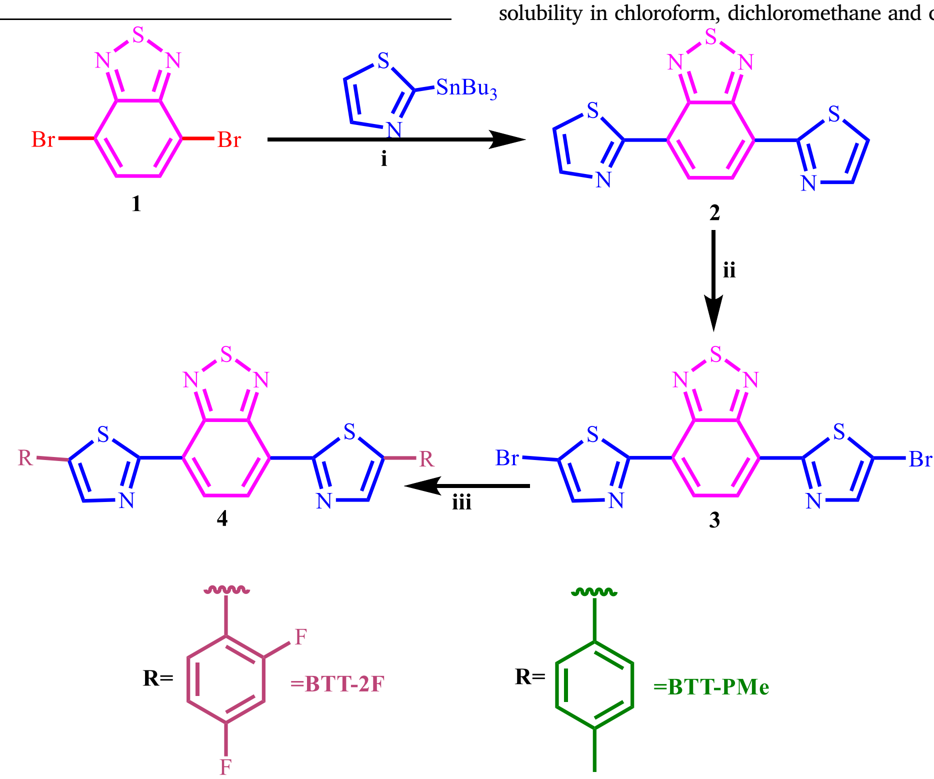

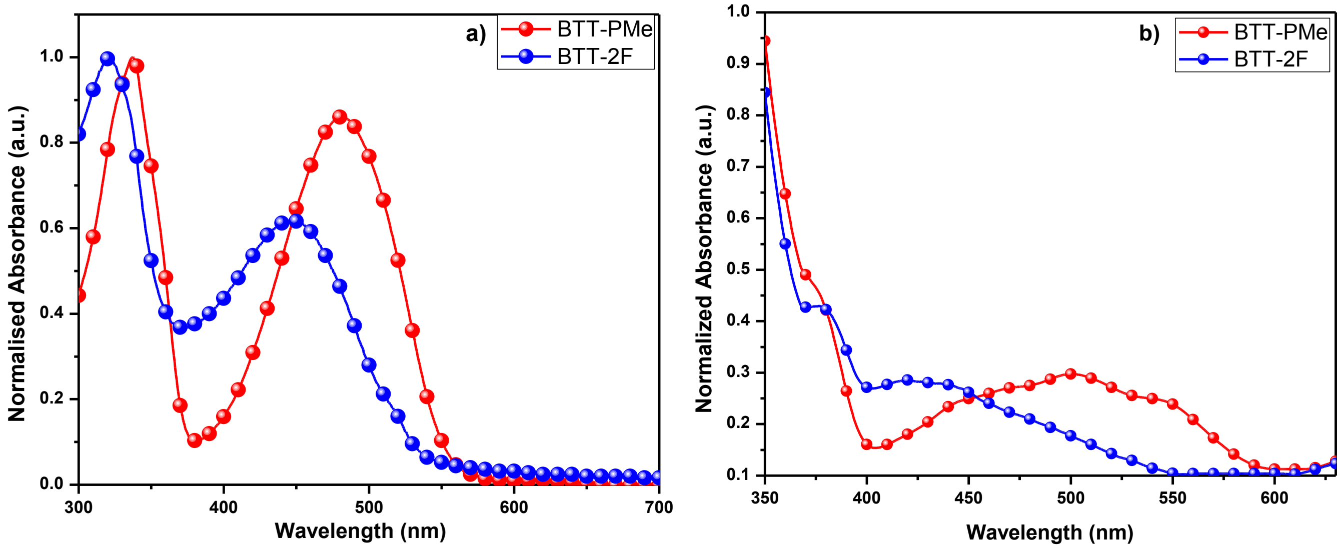

Fig. 2. Absorption spectra of **BTT-PMe** and **BTT-2F** in (a) chloroform solution (b) on film.

Table 1
Photophysical and electrochemical properties of **BTT-PMe** and **BTT-2F**.

HTMs	λ_{max} [nm][a]/ λ_{emi}[nm]	$M^{-1}cm^{-1}(\varepsilon)$[a]	HOMO [eV][b]	$E_{0\text{-}0}$ [eV][c]	LUMO [eV][b]
BTT-PMe	480/597	26,907	−5.55	2.29	−3.26
BTT-2F	450/560	7775	−5.58	2.48	−3.10

[a] Absorption spectra were recorded in $CHCl_3$ solution at 298 K.
[b] HOMO values were measured from CV by adding 4.8 to E_{oxd}.
[c] The bandgap ($E_{0\text{-}0}$) was calculated from the intersection point of the absorption and emission spectra.

Synthetic Scheme: Reagents and Conditions: (i) 2-(tributylstannyl) thiazole, Pd[PPh$_3$]$_4$, toluene, 70% yield, (ii) NBS, DMF, 80%Yield, (iii) a. 2 4-difluorophenylboronic acid OR p-methyl phenyl boronic acid, Pd [PPh$_3$]$_4$, Na_2CO_3, toluene, 100 °C, 60% yield.

4.2. Synthesis of the 2,3 and 4

We have prepared the compound 2,3 and 4 by previous reported literature. (Swetha et al., 2018)

4.3. Synthesis of the BTT-2F

A mixture of **4** (57 mg, 0.123 mmol), 2,4-difluorophenylboronic acid pinacol ester (98 mg, 0.119 mmol), Pd(PPh$_3$)$_4$ (7.9 mg), and Na_2CO_3 (39.3 mg, 3 mmol) was dissolved in toluene and water (3:1), the mixture was refluxed for 24 h. After completion of the reaction the toluene was evaporated by using the rota evaporator, then the mixture was poured into ice-water and extracted with DCM. The organic layer was dried with Na_2SO_4 and the solvent was evaporated in vacuo. The product was purified by column chromatography. Yield: 60%. ^{1}H NMR (400 MHz, $CDCl_3$, δ):7.70–7.64 (m, 4H), 7.56–7.53 (m, 2H), 7.50–7.45 (m, 4H). ESI-MS (*m/z*): 565 (M + K). FT-IR (KBr) (cm^{-1}): 3447, 3056, 2922, 1631, 1435, 1384, 1187, 1117, 758, 721, 693, 541, 501.

4.4. Synthesis of the BTT-PMe

The BTT-PMe was synthesized by using above procedure with the P-tolyl boronic acid in the place of 2,4-difluorophenylboronic acid pinacol ester. Yield: 60%. ^{1}H NMR (400 MHz, $CDCl_3$, δ): 8.73 (s, 2H), 8.18 (s, 2H) 7.64–7.61 (dd, 4H), 7.10–7.27 (m, 4H), 2.41 (s, 6H), ESI-MS (*m/z*): 483 (M + H). FT-IR (KBr) (cm^{-1}): 3754, 3448, 2921, 2853, 1630, 1513, 1468, 1376, 1265, 1159, 1122, 1074, 867, 807, 755, 717, 652, 565, 496, 407.

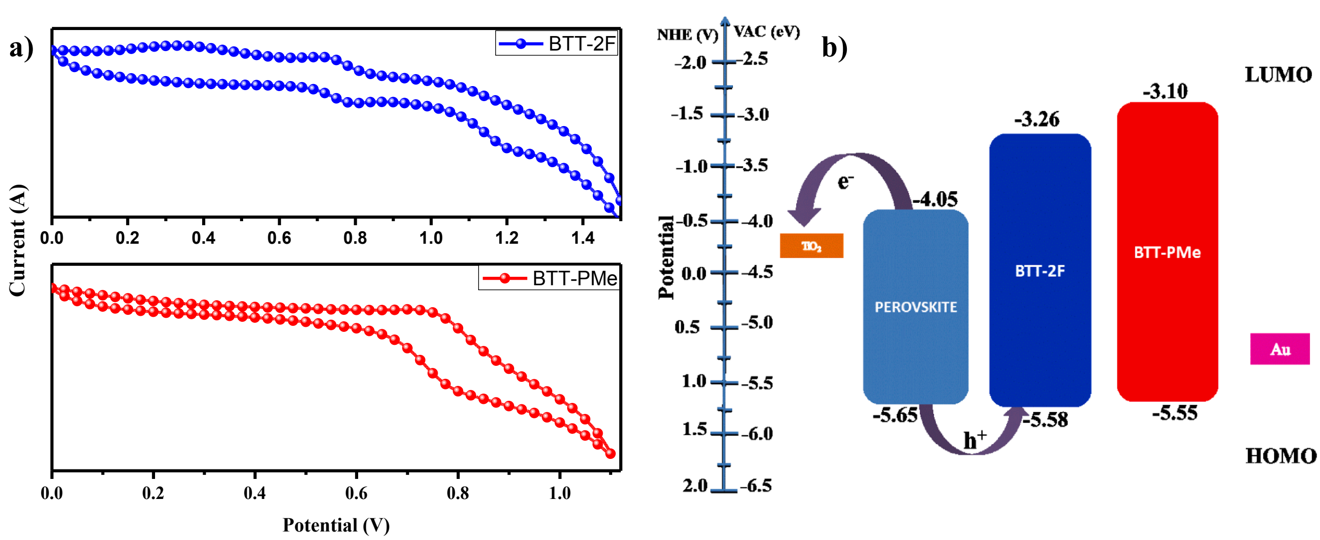

Fig. 3. (a) Cyclic voltammetry and (b) schematic energy levels of **BTT-2F, BTT-PMe** in chloroform *vs* NHE.

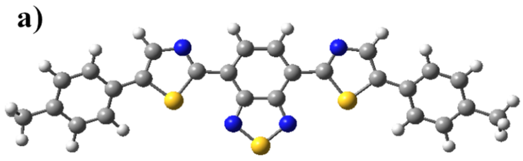

Fig. 4. Optimized structures of the (a) **BTT-PMe** and (b) **BTT-2F.**

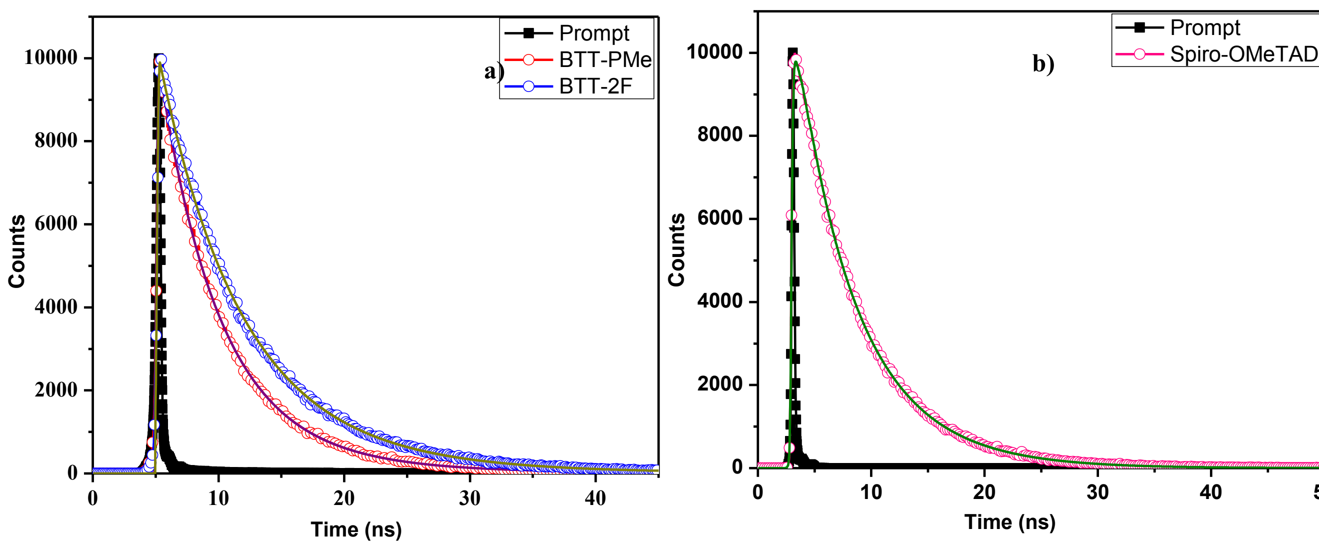

Fig. 5. TCSPC studies of dyes (a) **BTT-PMe** and **BTT-2F** using 440 nm laser excitation **(b) Spiro-OMeTAD** under 484 nm in chloroform solution. The hollow solid square represents the decay pattern and the solid circles symbolize the appropriate results.

Table 2
Decay parameter of the new HTMs.

HTMs	BTT-PMe	BTT-2F	Spiro-OMeTAD
τ_1 (ns)	0.45 ns (75.27%)	0.61 ns (69.04%)	0.33 ns (12.59%)
τ_2 (ns)	0.88 ns (24.73%)	1.01 ns (30.96%)	0.60 ns (87.41)
χ^2	1.30	1.29	1.03

4.5. Photophysical and electrochemical properties

The photophysical properties of new HTMs **BTT-2F** and **BTT-PMe** have recorded by the UV–Vis and photoluminiscence spectroscopy in chloroform solution. The UV–Vis absorption spectra in solution and on film have been shown in Fig. 2a and 2b and data were tabulated in Table 1. The absorption range of the synthesised **BTT-PMe** and **BTT-2F** were observed from 350 nm to 550 nm. The intramolecular charge transfer (ICT) maxima (λ_{max}) was centred at 480 nm, 450 nm with the molar extinction coefficient (ε) 26,907 M^{-1} cm^{-1} and 7775 M^{-1} cm^{-1} respectively. The high energy absorption bands found at the 320 nm, which is raised from the localized π-π* transitions. The limited absorption of these HTMs in the visible range will not interfere with the produced photocurrent of perovskite, which was araised by the strong absorption of the perovskite and leads toward the improvement of the photovoltaic properties. The same patterned absorption bands were observed in the thin film state (Fig. 2b), with the slightly red-shifted of the **BTT-PMe** suggesting that there is J-type aggregation. In **BTT-2F** it was blue-shifted because of the poor film quality (Wu et al., 2017).

The optimized geometries, frontier orbitals and simulated absorption data are provided in Supporting Information (Fig. S1). The absorption spectra for all the considered species of the HTMs have been computed and compared with the experimental data. The results were reported in Tables S1 and S2.

The TD-DFT calculations of **BTT-PMe** and **BTT-2F** revels that the intensive transistors S0 → S1 calculated at 479 nm from the HOMO-LUMO with the oscillator strength (*f*) = 1.2058 and 472 nm, which originates from the HOMO-LUMO with *f* = 1.190).

To know the suitability of the material for the hole transfer from the perovskite to HTM, the highest occupied molecular orbital (HOMO) of the HTM is playing a vital role. To know the suitability of the material for the hole transfer, we have calculated the HOMO energy level from the cyclic voltammetry (CV), which is performed with 0.1 M $[(CH_3CH_2)_4N]ClO_4$ as supporting electrolyte in chloroform solution and voltammograms are shown in Fig. 3a and energy level diagram represented in Fig. 3b. The relative data was tabulated in Table 1. The HOMO level of the **BTT-PMe** and **BTT-2F** were observed at −5.55 eV and −5.58 eV *vs* NHE, that are well-matched with the valence band of the perovskite (5.65 ev) (Xu et al., 2017) and energetically favorable for the hole injection at the interface. The lowest unoccupied molecular orbital (LUMO) was calculated by the $E_{LUMO} = E_{HOMO}$-$E_{0\text{-}0}$, where $E_{0\text{-}0}$ is zeroth-zeroth transition value, calculated from the intersection of normalized absorption and emission spectra. The LUMO energy levels of the **BTT-PMe** and **BTT-2F** was −3.26 eV and −3.10 eV respectively. The higher LUMO of these HTMs effectively inhibits the undesired photo-generated electron back transfer from the perovskite to the Au electrode (see Fig. 3b).

To further understand the optical properties in depth we have carried out the DFT studies of **BTT-PMe** and **BTT-2F**. The optimized structures of the BTT-PMe and BTT-2F are showed in the Fig. 4. HOMO is mainly contributed from the core to the arms and LUMO is located on the core of the HTMs. The frontier molecular orbital and the percentage contribution of each group to molecular orbital were shown in Tables S3 and S4. We have made the two fragments of the **HTM**s as benzo for benzodithiazole and terminal groups 2F for **BTT-2F** and PMefor **BTT-PMe**. Experimental, calculated λ_{max}, (nm) and HOMO, LUMO values of **BTT-PMe** and **BTT-2F** in chloroform solvent, shown in Table S5.

In the **BTT-2F** casethe HOMO, HOMO-1, HOMO-2 is distributed mainly on the benzo group (72%, 51% and 41%) and 28%, 49% and 59% on the terminal group 2F respectively**.** The HOMO-3 is located majorly on 2F (99%) compared to the benzo group (1%). On the benzo group, the major contribution occurs from the LUMO, LUMO + 1 and LUMO + 2 (91%, 81% and 59% respectively) because of the electron defecient nature and minorly from the 2F group (9%, 19% and 41%). The LUMO + 3 differs from them, the more distribution on the 2F (77%) and less on the benzo (23%). In **BTT-2F.**The HOMO, HOMO-1, HOMO-2 are localized on the PMe (~60%) and ~40% from the benzo group and HOMO-3 is dispersed mainly on the benzo ~80% and a small amount on P-Me (~20%).

To know the fluoroscence properties, we have performed TCSPC studies for the new HTMs (Fig. 5a) and state-of-the art *Spiro*-OMeTAD (Fig. 5b) in the chloroform solution at 440 nm and 484 nm excitation. The observed decays are well described using a bi-exponential function instead of the single exponential may be due to the presence of the two prominent generated carriers. The observed lifetime and amplitude values were summarized in the Table 2. The long lived component (τ_1) 0.45 ns, 0.61 ns with amplitude 75.27%, 69.04%, the short lived decay (τ_2) is 0.88 ns, 1.01 ns with amplitude 24.73%, 30.96% for **BTT-PMe**, **BTT-2F** respectively, which have the long life time compare to Spiro-OMeTAD showed the τ_1 is 0.33 ns and τ_2 is 0.60 ns.

5. Conclusion

In conclusion, we havepresent the synthesis and characterizationof novel benzodithiazole based simple HTMs **BTT-PMe** and **BTT-2F** for the high efficient PSCs. The theoretical studies are well-matched with experimental details. The **BTT-2F** showed the less molar extinction coefficient compares to the **BTT-PMe** because of poor film quality. The energy level of these HTMs are well aligned with perovskite to achieve good PCE.

Declaration of competing interest

The authors declare that they have no known competing financial interests or personal relationships that could have appeared to influence the work reported in this paper.

Acknowledgements

TS acknowledge support from Department of Science and Technology, SERB for National Postdoc Fellowship (Ref. No. PDF/2018/000880).This study was financially supported by the Dana Impak Perdana Research Scheme (Code: DIP-2018-019) of the Universiti Kebengsaan Malaysia (UKM). The authors also extend their appreciation to the Deanship of Scientific Research at King Saud University for supporting this work through research group NO (RGP-1440-102).

Appendix A. Supplementary material

Details about the analysis data (NMR, Mass Spectra) of HTMs and Computational Details. Supplementary data to this article can be found online at https://doi.org/10.1016/j.solener.2019.10.046.

References

Ahmed, G.H., El-Demellawi, J.K., Yin, J., Pan, J., Velusamy, D.B., Hedhili, M.N., Alarousu, E., Bakr, O.M., Alshareef, H.N., Mohammed, O.F., 2018. Giant photoluminescence enhancement in cspbcl3 perovskite nanocrystals by simultaneous dual-surface passivation. ACS Energy Lett. 3 (10), 2301–2307.

Bi, D., Tress, W., Dar, M.I., Gao, P., Luo, J., Renevier, C., Schenk, K., Abate, A., Giordano, F., Baena, J.P.-C., Decoppet, J.-D., Zakeeruddin, S.M., Nazeeruddin, M.K., Grätzel, M., Hagfeldt, A., 2016. Efficient luminescent solar cells based on tailored mixed-cation perovskites. Sci. Adv. 2, e1501170.

Chen, H., Bryant, D., Troughton, J., Kirkus, M., Neophytou, M., Miao, X., Durrant, J.R., McCulloch, I., 2016. One-step facile synthesis of a simple hole transport material for efficient perovskite solar cells. Chem. Mater. 28 (8), 2515–2518.

Chen, H., Bryant, D., Troughton, J., Kirkus, M., Neophytou, M., Miao, X., Durrant, J.R., McCulloch, I., 2016.

Cheng, M., Chen, C., Aitola, K., Zhang, F., Hua, Y., Boschloo, G., Kloo, L., Sun, L., 2016. Highly efficient integrated perovskite solar cells containing a small molecule-pc70bm bulk heterojunction layer with an extended photovoltaic response up to 900 nm. Chem. Mater. 28, 8631–8639.

Cheng, M., Li, Y., Safdari, M., Chen, C., Liu, P., Kloo, L., Sun, L., 2017. Efficient perovskite solar cells based on a solution processable nickel(ii) phthalocyanine and vanadium oxide integrated hole transport layer. Adv. Energy Mater. 7, 1602556.

Cheng, Chen, Xingdong, D., Hong Ping, L.I., Ming, Cheng, Henan, L.I., Li, Xu, Fen, Q., Huaming, L.I., 2018. Highly efficient phenoxazine core unit based hole transport materials for hysteresis-free perovskite solar cell. ACS Appl. Mater. Interfaces 104, 36608–36614.

Correa-Baena, J.-P., Abate, A., Saliba, M., Tress, W., Jacobsson, T.J., Grätzel, M., Hagfeldt, A., 2017. The rapid evolution of highly efficient perovskite solar cells. Energy Environ. Sci. 10 (3), 710–727.

Frisch, M., Trucks, G., Schlegel, H., Scuseria, G., Robb, M., Cheeseman, J., Montgomery Jr, J., Vreven, T., Kudin, K., Burant, J., 2003. Revision B. Gaussian. Inc., Pittsburgh PA. Grisorio, R., Roose, B., Colella, S., Listorti, A., Suranna, G.P., Abate, A., 2017.

Gao, P., Grätzel, M., Nazeeruddin, M.K., 2014. Organohalide lead perovskites for photovoltaic applications. Energy Environ. Sci. 7, 2448–2463.

Grisorio, R., Roose, B., Colella, S., Listorti, A., Suranna, G.P., Abate, A., 2017. Molecular tailoring of phenothiazine-based hole-transporting materials for high-performing perovskite solar cells. ACS Energy Lett. 2, 1029–1034.

Kojima, A., Teshima, K., Shirai, Y., Miyasaka, T., 2009. Organometal halide perovskites as visible-light sensitizers for photovoltaic cells. J. Am. Chem. Soc. 131 (17), 6050–6051.

Leijtens, T., Ding, I.-K., Giovenzana, T., Bloking, J.T., McGehee, M.D., Sellinger, A., 2012. Hole transport materials with low glass transition temperatures and high solubility for application in solid-state dye-sensitized solar cells. ACS Nano 6, 1455–1462.

Leijtens, T., Bush, K., Cheacharoen, R., Beal, R., Bowring, A., McGehee, M.D., 2017. Towards enabling stable lead halide perovskite solar cells; the interplay between structural, environmental, and thermal stability. J. Mater. Chem. A 5 (23), 11483–11500.

Miertuš, S., Scrocco, E., Tomasi, J., 1981. Electrostatic interaction of a solute with a continuum. A direct utilization of AB initio molecular potentials for the prevision of solvent effects. Chem. Phys. 55 (1), 117–129.

Molina-Ontoria, A., Zimmermann, I., Garcia-Benito, I., Gratia, P., Roldan-Carmona, C., Aghazada, S., Graetzel, M., Nazeeruddin, M.K., Martin, N., 2016. Benzotrithiophene-based hole-transporting materials for 18.2% perovskite solar cells. Angew. Chem. Int. Ed. 55, 6270–6274.

Petrus, M.L., Bein, T., Dingemans, T.J., Docampo, P., 2015. A Low-Cost azomethine-based hole transporting material for perovskite photovoltaics. J. Mater. Chem. A 3, 12159–12162.

Qin, P., Tanaka, S., Ito, S., Nicolas, T., Kyohei, M., Hitoshi, N., Nazeeruddin, M.K., Grätzel, M., 2014. Inorganic hole conductor-based lead halide perovskite solar cells with 12.4% conversion efficiency. Natute 5, 3834–3839.

Rakstys, K., Saliba, M., Gao, P., Gratia, P., Kamarauskas, E., Paek, S., Jankauskas, V., Nazeeruddin, M.K., 2016. Highly efficient perovskite solar cells employing an easily attainable bifluorenylidene-based hole-transporting material. Angew. Chem. Int. Ed. 55, 7464–7468.

Sepalage, G.A., Meyer, S., Pascoe, A., Scully, A.D., Huang, F., Bach, U., Cheng, Y.-B., Spiccia, L., 2015. Adv. Funct. Mater. 25, 5650.

Swetha, T., Akhtaruzzaman, M., Chowdhury, T.H., Amin, N., Islam, A., Noda, T., Upadhyaya, H.M., Singh, S.P., 2018. Benzodithiazole-based hole-transporting material for efficient perovskite solar cells. Asian J. Org. Chem. 7 (12), 2497–2503.

Tingwei, Z., Yubo, Z., Ming, W., Zhigang, Z., Xiaosheng, T., Liang, F., 2019. Two-dimensional lead-free hybrid halide perovskite using superatom anions with tunable electronic properties. Sol. Energy Mater. Sol. Cells 191, 33–38.

Tingwei, Z., Yubo, Z., Ming, W., Zhigang, Z., Xiaosheng, T., 2019. Tunable electronic structures and high efficiency obtained by introducing superalkali and superhalogen into AMX3-type perovskites. J. Power Sources 429 (31), 120–126.

Tingwei, Z., Yubo, Z., Ming, W., Zhigang, Z., Liang, F., 2019. Stable dynamics performance and high efficiency of abx3-type super-alkali perovskites first obtained by introducing h5o2 cation. Adv. Energy Mater. 1900664–1900672.

Wu, F., Ji, Y., Zhong, C., Liu, Y., Tan, L., Zhu, L., 2017. Fluorine-substituted benzothiadiazole-based hole transport materials for highly efficient planar perovskite solar cells with a FF exceeding 80%. Chem. Commun. 53 (62), 8719–8722.

Xiaofeng, Z., Tingwei, Z., Chongqian, Leng, Zhigang, Z., Ming, W., Wei, H., Xiaosheng, T., Shirong, L., Liang, F., Miao, Z., 2017. Performance improvement of perovskite solar cells by employing a CdSe quantum dot/PCBM composite as an electron transport layer. J. Mater. Chem. A 5, 17499–17505.

Xu, B., Zhang, J., Hua, Y., Liu, P., Wang, L., Ruan, C., Li, Y., Boschloo, G., Johansson, E.M.J., Kloo, L., Hagfeldt, A., Jen, A.K.-Y., Sun, L., 2017. Tailor-making low-cost spiro [fluorene-9,9'-xanthene]-based 3d oligomers for perovskite solar cells. Chem 2, 676–687.

Ye, Senyun, Sun, Weihai, Li, Yunlong, Yan, Weibo, Peng, Haitao, Bian, Zuqiang, Liu, Zhiwei, Huang, Chunhui, 2015. CuSCN-based inverted planar perovskite solar cell with an average PCE of 15.6%. Nano Lett. 15 (6), 3723–3728. https://doi.org/10.1021/acs.nanolett.5b00116.